ARTICLES
PUBLISHED ONLINE: 12 FEBRUARY 2012 | DOI: 10.1038/NPHOTON.2011.356
nature photonics

Tandem polymer solar cells featuring a spectrally matched low-bandgap polymer

Letian Dou[1‡], Jingbi You[1‡], Jun Yang[1], Chun-Chao Chen[1], Youjun He[1], Seiichiro Murase[1†], Tom Moriarty[2], Keith Emery[2], Gang Li[1] and Yang Yang[1,3]*

Tandem solar cells provide an effective way to harvest a broader spectrum of solar radiation by combining two or more solar cells with different absorption bands. However, for polymer solar cells, the performance of tandem devices lags behind single-layer solar cells mainly due to the lack of a suitable low-bandgap polymer. Here, we demonstrate highly efficient single and tandem polymer solar cells featuring a low-bandgap conjugated polymer (PBDTT-DPP: bandgap, ~1.44 eV). A single-layer device based on the polymer provides a power conversion efficiency of ~6%. When the polymer is applied to tandem solar cells, a power conversion efficiency of 8.62% is achieved, which is, to the best of our knowledge, the highest certified efficiency for a polymer solar cell to date.

Organic photovoltaic (OPV) devices show great promise in low-cost, flexible, lightweight, large-area, energy-generation applications[1–12], and much work on designing new materials[10,13–18], device structures[19–23] and processing techniques[24–26] has been carried out to improve the power conversion efficiency (PCE) of such devices. So far, polymer solar cells (PSCs) based on conjugated polymers as electron-donor materials blended with [6,6]-phenyl-C_{71}-butyric acid methyl ester ($PC_{71}BM$) as an electron-acceptor material have achieved ~8% PCE using a bulk heterojunction (BHJ) device structure[27–31]. However, most of these materials suffer from the inherent disadvantages of either lacking a broad absorption range (bandgap [E_g] ≈ 1.6–2.0 eV), which limits the use of the full solar spectrum, or having a relatively low carrier mobility, which requires the use of thinner films for efficient charge extraction[13–18,27,31]. This reduces the external quantum efficiency (EQE) and photocurrent of the devices. To use solar radiation more effectively, one approach is to stack, in series, multiple photoactive layers with complementary absorption spectra to construct a tandem PSC[6–9]. In a typical double-junction cell, such a tandem structure consists of a front cell with a high-bandgap material, an interconnecting layer (ICL), and a rear cell comprising a low-bandgap material. When compared to a single-junction device made using low-bandgap materials, this tandem structure has a reduced photovoltage loss during the photon-to-electron conversion process. This is because the open-circuit voltage (V_{OC}) from a solar cell is fundamentally limited by the bandgap of the active materials, so by using more than one material, each of which captures a different part of the solar spectrum, V_{OC} is increased and also therefore the efficiency[1–9].

So far, most research carried out on tandem PSCs has focused on improving the ICL between two sub-cells and only a few cases have demonstrated high efficiency[6–9,32–34]. Photoactive materials play a critical role in determining the PCE. However, because of the great difficulties associated with making such materials, there have been few reports to date of photoactive materials designed specifically for high-efficiency tandem PSCs. To be used effectively in a tandem structure, sub-cell materials have several requirements, particularly in the creation of rear-cell low-bandgap polymers. First, a small energy bandgap (<1.5 eV) is critical so that overlap of absorption spectra between the front and rear cells can be minimized[34]. Second, fine-tuning is required for the highest-occupied molecular orbital (HOMO) and lowest-unoccupied molecular orbital (LUMO) levels to achieve a high V_{OC} with a small bandgap, while maintaining a LUMO level high enough for efficient charge separation[35]. Third, high charge carrier mobility and fine phase separation with the acceptor are required to achieve a high short-circuit current density (J_{SC}) and fill factor (FF) in single-cell devices[27–31]. Because the two cells are connected in series, the total current will be limited by the sub-cell with the lower current. Obtaining a high current in the rear cell is a great challenge, because most of the high-energy portion of the incident light will have already been absorbed by the front cell, so the current it can provide will be lower than in a single-cell device. Therefore, a carefully designed low-bandgap polymer will perform well in tandem cells only if it can achieve high current by efficiently using the low-energy portion of the solar spectrum. Existing low-bandgap materials (E_g < 1.5 eV) such as poly[2,6-(4,4-bis-(2-ethylhexyl)-4H-cyclopenta[2,1-*b*;3,4-*b*′] dithiophene)-alt-4,7-(2,1,3-benzothiadiazole)] (PCPDTBT), poly[(4, 4′-bis(2-ethylhexyl)dithieno[3,2-*b*:2′,3′-d]silole)-2,6-diyl-alt-(2,1,3-benzothiadiazole)-4,7-diyl] (PSBTBT) and poly[3,6-bis(4′-dodecyl-[2,2′]bithiophenyl-5-yl)-2,5-bis(2-ethylhexyl)-2,5-dihydro-pyrrolo[3,4-]pyrrole-1,4-dione] (pBBTDPP2) have either low V_{OC}, low J_{SC} or low FF values, which are far from ideal for the tandem structure. This means that the PCE of tandem cells reported to date is less than 7% (refs 6–9).

Low-bandgap polymer design

Here, we demonstrate the rational design of a novel low-bandgap conjugated polymer, poly{2,6′-4,8-di(5-ethylhexylthienyl)benzo[1,2-*b*;3,4-b]dithiophene-alt-5-dibutyloctyl-3,6-bis(5-bromothiophen-2-yl)pyrrolo[3,4-*c*]pyrrole-1,4-dione} (PBDTT-DPP, Fig. 1a), specifically for tandem solar cells. To achieve a small bandgap, a polymer backbone based on the diketopyrrolopyrrole (DPP) and benzodithiophene (BDT) units was chosen, inspired by a low-bandgap polymer

[1]Department of Materials Science and Engineering, University of California, Los Angeles, Los Angeles, California 90095, USA, [2]National Renewable Energy Laboratory, Golden, Colorado 80401, USA, [3]California NanoSystems Institute, University of California, Los Angeles, Los Angeles, California 90095, USA; [†]Present address: Toray Industries, Inc., Nihonbashi Mitsui Tower, 1-1, Nihonbashi-Muromachi 2-chome, Chuo-ku, Tokyo 103-8666, Japan; [‡]These authors contributed equally to this work. *e-mail: yangy@ucla.edu

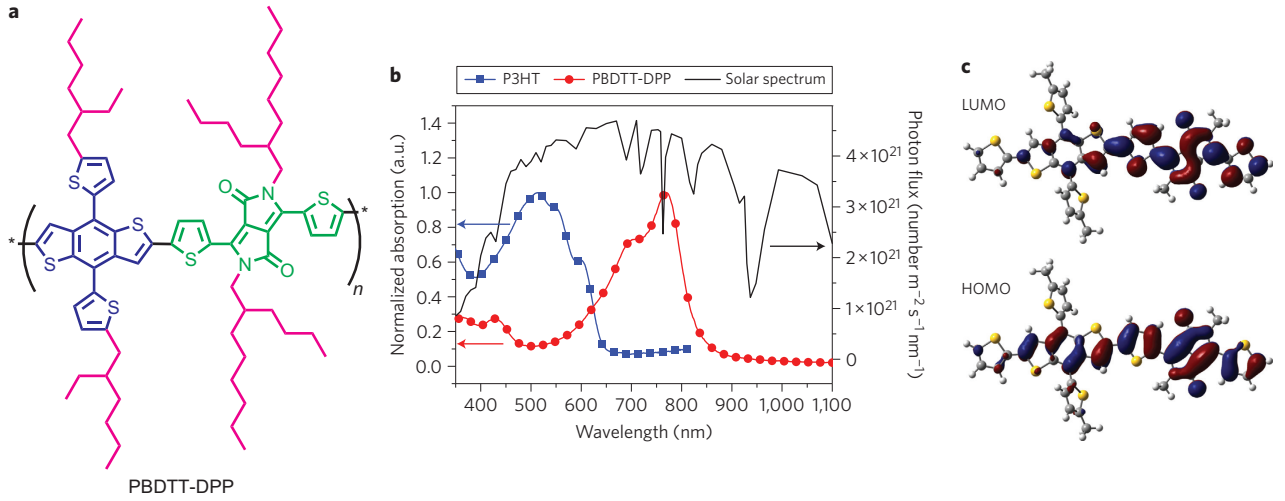

Figure 1 | Molecular design, optical properties and electron density of HOMO and LUMO for PBDTT-DPP. a, Chemical structure of PBDTT-DPP. **b**, UV-visible absorption spectra of PBDTT-DPP and P3HT films and the solar radiation spectrum. The UV-visible absorption profiles of PBDTT-DPP and P3HT show that the two materials cover the solar spectrum from 350 to 850 nm in a complementary manner. **c**, Electron density of HOMO and LUMO for PBDTT-DPP computed by density functional theory (DFT).

(PBDT-DPP) that we have previously reported to have a promising bandgap of 1.3 eV, although a rather disappointing photovoltaic performance[36]. By replacing the oxygen atoms attached to the BDT unit with thiophene moieties to form the thienylbenzodithiophene (BDTT) unit, the HOMO and LUMO levels of PBDTT-DPP are moved deeper to increase V_{OC} without losing the driving force for efficient charge separation[37], but the bandgap is kept within the ideal range. Furthermore, bulkier 2-ethylhexyl side chains on BDTT and 2-butyloctyl side chains on DPP are used to increase the solubility of the resulting polymers and thus obtain much higher molecular weights. Compared to PBDT-DPP, PBDTT-DPP has demonstrated improved solubility, higher molecular weight and higher carrier mobility, leading to a significantly higher J_{SC} in single-cell devices. With PBDTT-DPP, PCEs greater than 6% have been achieved in single-cell devices with both regular[19] and inverted[20–22] structures. Finally, we used this low-bandgap polymer in a newly designed inverted-structure tandem solar cell, and a PCE of 8.62% was certified by the National Renewable Energy Laboratory (NREL). It is important to point out that the measurement of tandem/multijunction organic solar cells is non-trivial. The single-junction cell measurement method[38], which is commonly used in tandem OPV research, can lead to significant errors in tandem cell measurements. A brief description of the correct procedure for tandem solar cell measurement is described in this Article.

Figure 1b presents the UV-visible absorption spectra of PBDTT-DPP and poly(3-hexylthiophene) (P3HT, $E_g \approx 1.9$ eV) in the solid state, as well as the solar radiation spectrum. The absorption onset of PBDTT-DPP is located at 858 nm, indicating an optical bandgap of 1.44 eV. When comparing the absorption spectra of PBDTT-DPP and P3HT (the most frequently used front-cell material), the overlap for the two materials can be seen to be small, meaning that they cover the solar spectrum from 350 to 850 nm in a complementary manner and are therefore a good match for building a tandem structure. Figure 1c reveals that the electron density of the LUMO for one repeating unit of PBDTT-DPP is almost entirely localized on the DPP unit, whereas that of the HOMO is distributed more evenly over the entire π-conjugated system. (The estimated bandgap and HOMO/LUMO from quantum chemical calculations for both PBDTT-DPP and PBDT-DPP can be found in the Supplementary Information.) The HOMO and LUMO energy levels for PBDTT-DPP were found to be −5.30 and −3.63 eV, and for PBDT-DPP were −5.16 and −3.51 eV, as determined by cyclic voltammetry (CV)[36]. A slightly higher energy bandgap was determined using CV (~1.6 eV) than from UV-visible absorption measurements (~1.4 eV), probably because of an energy barrier between the polymer film and electrode used in the CV measurement or because of the different binding energy of excitons created in the optical and electrochemical measurement[39]. (For details, see Supplementary Fig. S1.) A much deeper HOMO was obtained for PBDTT-DPP, suggesting a higher V_{OC} for BHJ solar cell devices combined with $PC_{71}BM$. The offset of the LUMO levels between PBDTT-DPP and $PC_{71}BM$ was slightly higher than the minimum value (~0.3 eV) for efficient charge separation at the interface of the donor and acceptor (the LUMO for $PC_{71}BM$ is −4.0 eV)[10]. We attribute this to the weaker electron-donating property of the theinyl group compared to the alkoxy group on the BDT unit (a similar effect has recently been observed in another polymer system[40]). The molecular weight (M_n) of PBDTT-DPP was found to be 40.7 kDa (compared with 8.5 kDa for PBDT-DPP). The much higher M_n of PBDTT-DPP was achieved by using bulkier side chains.

The hole mobilities of PBDT-DPP and PBDTT-DPP were determined by applying the space-charge limited current (SCLC) model[16,27] to the J–V measurements of the devices (see Supplementary Information). Supplementary Fig. S2 shows the $J^{0.5}$–V plots for the SCLC model. The hole mobilites were found to be 3.1×10^{-4} and 6.6×10^{-5} cm^2 V^{-1} s^{-1} for PBDTT-DPP and PBDT-DPP, respectively. Because the intermolecular packing distance is similar for PBDTT-DPP and PBDT-DPP, as indicated by X-ray diffraction studies (Supplementary Fig. S3)[31], the higher hole mobility for PBDTT-DPP is probably a result of its higher molecular weight[41].

Single-layer devices

Single-layer BHJ photovoltaic cells based on PBDTT-DPP blended with $PC_{71}BM$ were fabricated with a regular[19] and an inverted configuration[20–22]. The optimized polymer:$PC_{71}BM$ blend ratio (by weight) was found to be 1:2 (Supplementary Fig. S4) and the optimized film thickness was ~100 nm. The single-cell photovoltaic performance of PBDTT-DPP is shown in Fig. 2a. Of the more than 300 devices that were fabricated, the best devices gave the following values: $V_{OC} \approx 0.74$ V, $J_{SC} \approx 13.5$ mA cm^{-2}, FF ≈ 65%. PCE values as high as 6.5% were achieved for both regular and inverted structures; indeed, 90% of the devices gave PCE values over 6.0%.

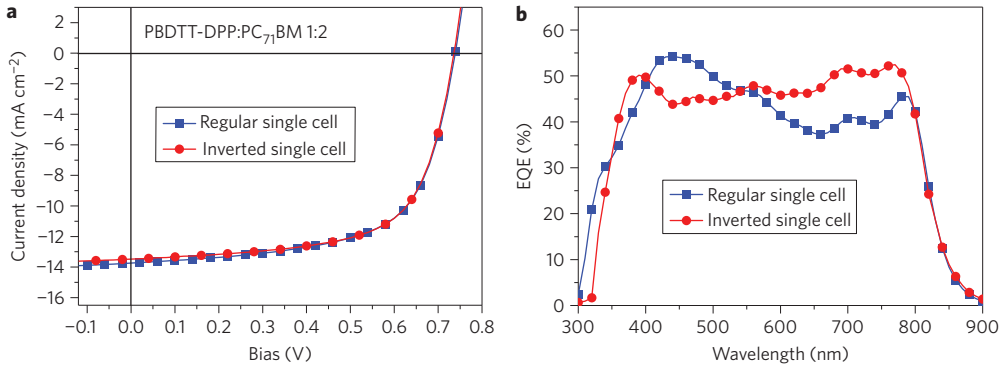

Figure 2 | *J–V* characteristics and EQEs of regular and inverted single-cell devices. a, *J–V* characteristics of single-cell devices with regular and inverted structures under AM1.5G illumination from a calibrated solar simulator with an irradiation intensity of 100 mW cm^{-2} (about one sun). **b**, EQE of the corresponding devices. Both regular and inverted single-cell devices show identical highest performances with $V_{OC} = 0.74$ V, $J_{SC} \approx 13.5$ mA cm^{-2}, FF $\approx 65\%$ and PCE $= 6.5\%$. The devices exhibit a very broad response range covering 350–850 nm.

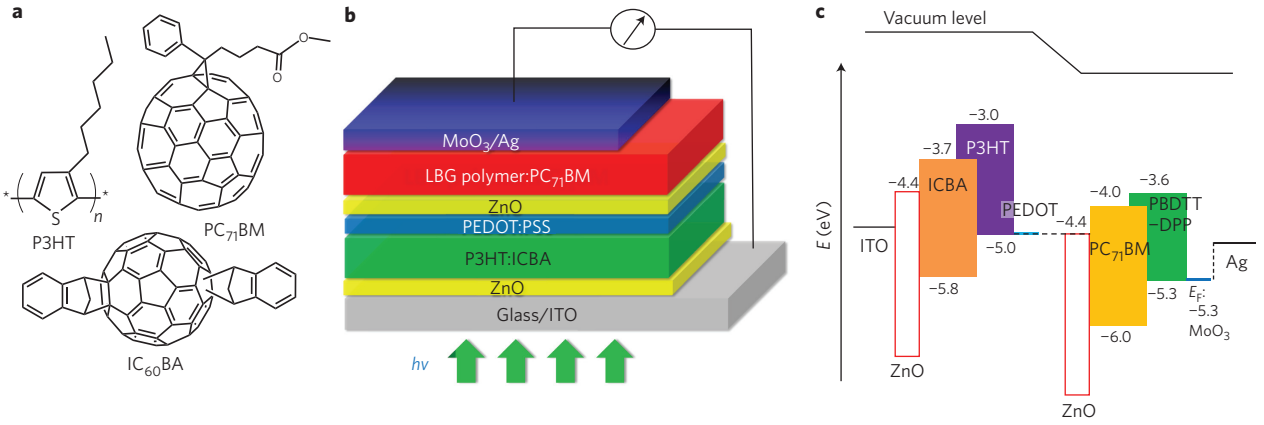

Figure 3 | Inverted tandem solar cells. a, Chemical structures of P3HT, $IC_{60}BA$ and $PC_{71}BM$. **b**, Device structure of the inverted tandem solar cell (LBG, low bandgap). **c**, Energy diagram of the inverted tandem devices.

All the parameters that determine overall performance were dramatically better than those achieved using the previous low-bandgap polymer, PBDT-DPP[36]. The increase in V_{OC} can be attributed to the deeper HOMO level, and the enhancement of J_{SC} and FF can be attributed to the higher hole mobility of PBDTT-DPP (the hole mobility of PBDTT-DPP:$PC_{71}BM$ with a 1:2 weight ratio was found to be 2.9×10^{-4} cm^2 V^{-1} s^{-1}, which is close to the pristine polymer, indicating that charge carrier transport is not disturbed by adding $PC_{71}BM$ into the polymer network; Supplementary Fig. S2). It is worth mentioning that compared to early efforts in inverted OPV devices, a very high FF (65%) is achieved here, which indicates that the interface materials have superior performance. Figure 2b shows the EQE for the corresponding single-junction devices, which exhibit broad response ranges covering 350–850 nm, with an average EQE of 47% within this region and a peak EQ of ~55%. These results indicate that the low-bandgap polymer successfully achieves high performance while maintaining a small bandgap.

Tandem devices

A detailed study was carried out on the tandem PSCs based on PBDTT-DPP. In our tandem structure, P3HT (a high-bandgap polymer) and the acceptor indene-C_{60} bisadduct ($IC_{60}BA$)[42] were selected as front-cell materials, and PBDTT-DPP together with the acceptor $PC_{71}BM$ were chosen as rear-cell materials. The corresponding chemical structures are shown in Fig. 3a. In this Article, the inverted tandem structure was chosen because of its advantages of a simple, robust device fabrication process and better stability[9,20–22]. The device structure and the corresponding energy diagram are shown in Fig. 3b,c. ZnO nanoparticles were used as the electron-transport material because their workfunction matches well with the acceptors and the high electron mobility[9]. PEDOT:PSS was used as the hole-transport material for P3HT, and MoO_3 was used for PBDTT-DPP because of their good workfunction aligment with the polymer and its high hole mobility[8,9]. Ultraviolet photoelectron spectroscopy was used to examine the workfunctions of the ICLs, including PEDOT:PSS and ZnO (Supplementary Fig. S5). The results were in accordance with reported data[8,9]. The energy difference between different layers was minimized by material selection to ensure good charge transport.

Inverted tandem solar cells were fabricated using the rear-cell-specific low-bandgap polymer PBDTT-DPP and the new device architecture. The *J–V* characteristics, EQE and performance parameters of a typical device are shown in Fig. 4 and Table 1 (EQE results measured at NREL were almost identical to those measured at the University of California, Los Angeles (UCLA) and can be found in Supplementary Fig. S6). The EQE of individual sub-cells in the tandem structure was measured using light bias, as first proposed by Burdick and Glatfelter[43] in the 1980s for inorganic multi-junction cells and more recently adopted by Kim and Janssen[6,44] in organic tandem solar cells (see Methods for details). As shown in Fig. 4a, the front cell had a photoresponse from 300 to 600 nm,

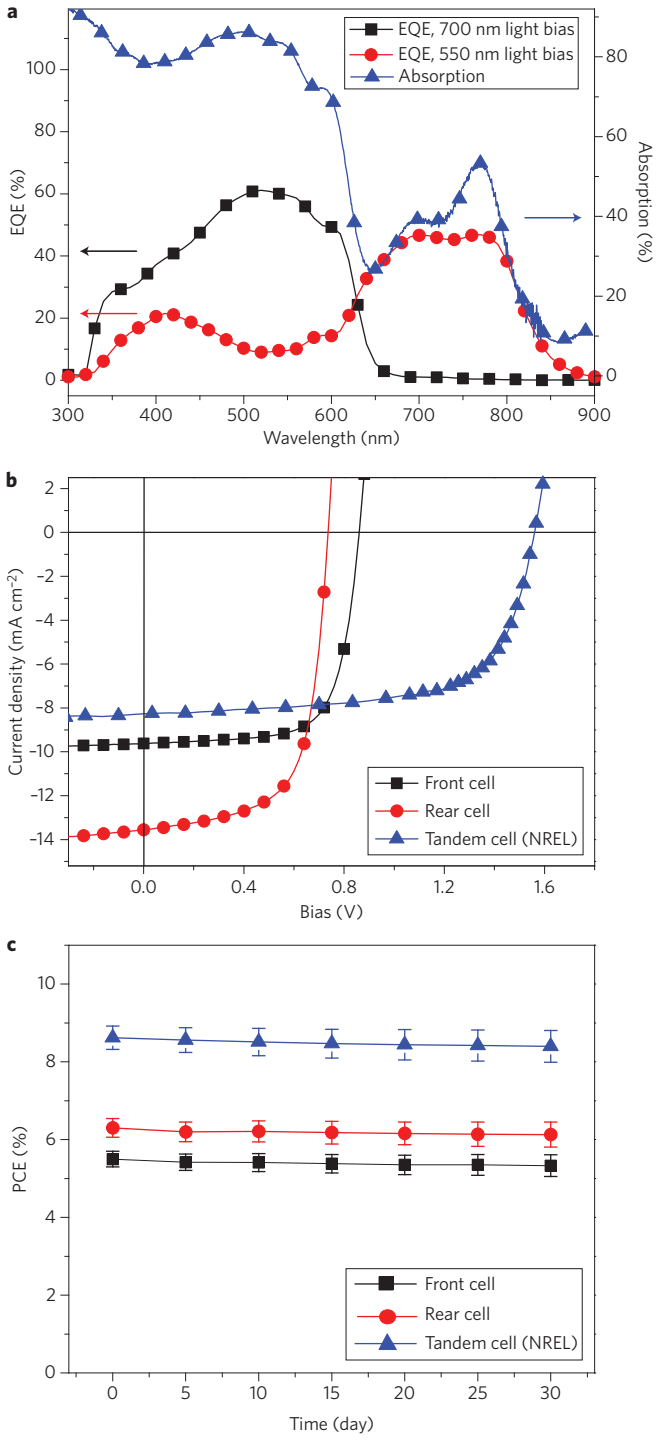

Figure 4 | Quantum efficiencies, *J–V* characteristics and stability of single cells and tandem cells. a, EQEs of the inverted tandem solar cell and absorption spectrum (without metal electrode). **b**, *J–V* characteristics of the front cell, rear cell and inverted tandem solar cell, tested at NREL using the OSMSS simulator. **c**, Stability of the inverted front cells, rear cells and tandem cells (tested at UCLA).

showed an EQE as high as 60% at 530 nm, and its integrated J_{SC} was 8.2 mA cm^{-2}. The rear cell had a broad photoresponse from 300 to 850 nm, showed a maximum EQE of 47% at 770 nm, and its integrated J_{SC} was 8.1 mA cm^{-2}. The incident light from 300 to 600 nm was strongly absorbed by the front cell, and the EQE of the rear cell in this region was much lower than that of its single-cell devices (Fig. 2b); however, the rear cell can still provide enough photocurrent (8.1 mA cm^{-2}) to match the current supplied by the front cell (8.2 mA cm^{-2}), because the new material, PBDTT-DPP, can very efficiently use the low-energy portion (from 600 to 850 nm) of the solar radiation.

Table 1 | Inverted single and tandem solar cell performance.

	V_{OC} (V)	J_{SC} (mA cm^{-2})	FF (%)	PCE (%)
Front cell	0.85	9.56	70.2	5.7
Rear cell	0.74	13.5	65.1	6.5
Tandem (NREL)	1.56	8.26	66.8	8.6
Tandem*	1.20–1.58	6.0–7.8	52.0–67.0	4.9–6.5

*Data reported in refs 5–8.

Tandem cell characterization

Accurate tandem cell measurement is much more complicated than single-junction cell measurement. Each device junction must behave the same under the simulator spectrum as it would have behaved under the reference spectrum (AM1.5G). This requires significant adjustment of the simulator spectrum, which is traditionally a tedious iterative process that involves calculating the spectral mismatch of each junction and changing the filter in each run. Based on the EQE results, our devices were measured using the One-Sun Multi-Source Simulator (OSMSS) recently established at NREL. This simulator uses nine separate wavelength bands of light to build a spectrum so that the ratio of current for the front cell under the reference spectrum and the simulator spectrum is the same as the ratio of current for the rear cell under the reference spectrum and the simulator spectrum. Once such a spectrum is established, the total irradiance is set with a primary calibrated reference cell. In this way, each device junction behaves the same under the simulator spectrum as it would have behaved under the reference spectrum.

The *J–V* curves of the two single-junction devices as front and rear cells (measured at UCLA) and the tandem cell (measured at NREL) are shown in Fig. 4b. The original certified *I–V* curve and experimental details of the tandem device tested by NREL are shown in Fig. 5. The tandem cell achieved a PCE of 8.62%. The J_{SC} is 8.26 mA cm^{-2} and V_{OC} is 1.56 V, which is expected as the addition of the V_{OC} of two sub-cells. An excellent FF of 66.8% is

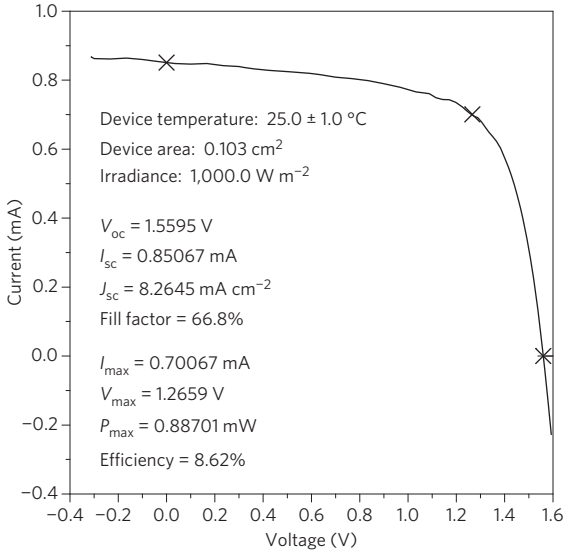

Figure 5 | Original *I–V* characteristics of the tandem device as measured by NREL.

achieved. To the best of our knowledge, this represents the highest certified efficiency in the OPV field. From the absorption spectrum of the tandem device (Fig. 4a), more than 80% of the solar radiation from 300 to 600 nm and only ~45% from 600 to 850 nm was absorbed. Therefore, by further increasing the absorption and EQE of the low-bandgap polymer-based rear cell, even higher PCEs could be achieved for the tandem solar cells. In addition to its high efficiency, our inverted device shows excellent reproducibility and stability. Of the 500 devices we fabricated, more than 300 showed PCEs around 8.5%. The devices maintain more than 95% of their original performance after encapsulation for 30 days (stored in a glovebox), as shown in Fig. 4c (24 samples were measured at UCLA).

In summary, we have demonstrated a high-performance low-bandgap conjugated polymer designed specifically for tandem PSCs by applying three rules: lowering the bandgap for spectral-matching with the front cell, controlling HOMO/LUMO levels to enhance V_{OC}, and increasing the molecular weight to enhance J_{SC} and FF. The novel polymer (PBDTT-DPP) has a small optical bandgap, deep HOMO level and high hole mobility. Single-layer BHJ solar cells fabricated from PBDTT-DPP and $PC_{71}BM$ exhibited PCEs of more than 6%. The significance of the PBDTT-DPP polymer is clearly demonstrated by the inverted tandem PSCs, which showed a PCE of 8.62% under AM1.5G one-sun illumination, as measured by NREL. This study opens up a new direction for polymer chemists to pursue in the design of new materials for tandem PSCs, and also represents an important step forwards in the commercialization of PSCs.

Methods

Materials. PBDTT-DPP, PBDT-DPP and $IC_{60}BA$ were synthesized at UCLA (see Supplementary Information). P3HT was purchased from Rieke Metals. $PC_{71}BM$ was purchased from Nano-C. Unless otherwise stated, all chemicals were purchased from Aldrich and used as received.

Tandem device fabrication. The device architecture of the tandem solar cell is shown in Fig. 3b. Pre-cleaned indium tin oxide (ITO) substrates were treated with UV-ozone. P3HT:$IC_{60}BA$ (1:1 weight ratio) in 1.8% 1,2-dichlorobenzene (DCB) solution was spin coated at 800 r.p.m. for 30 s on top of a layer of ZnO. The synthesis process for the ZnO nanoparticles can be found in refs 45 and 46. The films were annealed at 150 °C for 10 min. PEDOT:PSS (modified using the method described in ref. 33) was spin-coated on the first active layer and annealed at 150 °C for 10 min. A thin layer of ZnO film was then spincast, followed by thermal annealing at 150 °C for 10 min. Subsequently, PBDTT-DPP:$PC_{71}BM$ (1:2) from an 8 mg ml^{-1} DCB solution was spin-coated without any processing. Device fabrication was completed by thermal evaporation of 15 nm MoO_3 and 100 nm silver (as the anode) under vacuum at a base pressure of 2×10^{-6} torr. The effective area of the film was measured to be ~0.10 cm^2.

Single-junction device measurement. The fabricated devices were encapsulated in a nitrogen-filled glovebox using UV epoxy and cover glass. The current density/voltage curves were measured using a Keithley 2400 source-measure unit. Photocurrent was measured under AM1.5G illumination at 100 mW cm^{-2} using a Newport Thermal Oriel 91192 1000 W solar simulator. Light intensity was determined by KG-5 filter diodes (traceable to NREL calibration) as a reference cell, followed by calculation of a spectral mismatch factor and then short-circuit current (J_{SC}) correction. EQEs were measured using a lock-in amplifier (SR830, Stanford Research Systems) with a current preamplifier (SR570, Stanford Research Systems) under short-circuit conditions. The devices were illuminated using monochromatic light from a xenon lamp passing through a monochromator (SpectraPro-2150i, Acton Research Corporation) with a typical intensity of 10 μW. The photocurrent signal was amplified by the SR570 preamplifier and detected with an SR830 device. A calibrated monosilicon diode with a known spectral response was used as a reference.

Tandem device measurement. Device areas were measured in the NREL facility, and ranged from 0.0998 to 0.104 cm^2. EQEs were first measured at UCLA using the same EQE set-up as above. A 550 and 700 nm light bias was selected to excite the front and rear cells to measure the EQE of the rear and front cells, respectively. It should be noted that EQE measurements using this method are appropriate only for cases in which the two sub-cells exhibit a large enough shunt resistance. Otherwise, an electrical bias should be applied to avoid overestimation[39,47]. Here, the shunt resistances for the front, rear and tandem cells are as high as 2.25×10^5, 1.37×10^5 and 3.98×10^5 Ω cm^2, respectively (calculated from I–V measurements under dark conditions; see Supplementary Fig. S7). Therefore, EQE measurements using light bias only were conducted, and the J_{SC} from the EQE could be derived. I–V measurements for the tandem organic cells were performed on the OSMSS and were measured by NREL using quantum efficiencies provided by UCLA for spectral mismatch correction. EQEs were re-measured at NREL, and the spectral mismatches associated with the re-measured EQEs and the simulator spectra were recalculated. In each case, the spectral mismatches differed by less than 0.1% from those derived from the EQEs. Measurements were carried out at 1,000, 500 and 250 W m^{-2} with and without the mask (~0.04 cm^2) on a representative device. The J_{SC} with the mask was ~2% lower than without the mask. Some of this difference is probably due to the extended source of the OSMSS light (as opposed to a point-like source) and the thickness of the mask relative to the size or the opening.

Received 31 August 2011; accepted 14 December 2011; published online 12 February 2012

References

1. Würfel, W. *Physics of Solar Cells* (Wiley-VCH, 2005).
2. King, R. R. *et al.* 40% efficient metamorphic GaInP/GaInAs/Ge multijunction solar cells. *Appl. Phys. Lett.* **90,** 183516 (2007).
3. Wang, X. H., *et al.* Tandem colloidal quantum dot solar cells employing a graded recombination layer. *Nature Photon.* **5,** 480–484 (2011).
4. Riede, M. *et al.* Efficient organic tandem solar cells based on small molecules. *Adv. Funct. Mater.* **21,** 3019–3028 (2011).
5. Xue, J., Uchida, S., Rand, B. P. & Forrest, S. R. Asymmetric tandem organic photovoltaic cells with hybrid planar-mixed molecular heterojunctions. *Appl. Phys. Lett.* **85,** 5757–5759 (2004).
6. Kim, J. Y. *et al.* Efficient tandem polymer solar cells fabricated by all-solution processing. *Science* **317,** 222–225 (2007).
7. Gilot, J., Wienk, M. M. & Janssen, R. A. J. Optimizing polymer tandem solar cells. *Adv. Mater.* **22,** E67–E71 (2010).
8. Sista, S. *et al.* Highly efficient tandem polymer photovoltaic cells. *Adv. Mater.* **22,** 380–383 (2010).
9. Chou, C. H. *et al.* Metal-oxide interconnection layer for polymer tandem solar cells with an inverted architecture. *Adv. Mater.* **23,** 1282–1286 (2011).
10. Cheng, Y. J., Yang, S. H. & Hsu, C. S. Synthesis of conjugated polymers for organic solar cell applications. *Chem. Rev.* **109,** 5868–5923 (2009).
11. Coakley, K. M. & McGehee, M. D. Conjugated polymer photovoltaic cells. *Chem. Mater.* **16,** 4533–4542 (2004).
12. Brabec, J., Sariciftci, N. S. & Hummelen, J. C. Plastic solar cells. *Adv. Funct. Mater.* **11,** 15–26 (2001).
13. Boudreault, P. T., Najari, A. & Leclerc, M. Processable low-bandgap polymers for photovoltaic applications. *Chem. Mater.* **23,** 456–469 (2011).
14. Zhu, Z. *et al.* Panchromatic conjugated polymers containing alternating donor/acceptor units for photovoltaic applications. *Macromolecules* **40,** 1981–1986 (2007).
15. Hou, J. *et al.* Synthesis, characterization, and photovoltaic properties of a low band gap polymer based on silole-containing polythiophenes and 2,1,3-benzothiadiazole. *J. Am. Chem. Soc.* **130,** 16144–16145 (2008).
16. Liang, Y. Y., *et al.* Highly efficient solar cell polymers developed via fine-tuning of structural and electronic properties. *J. Am. Chem. Soc.* **131,** 7792–7799 (2009).
17. Bijleveld, J. C. *et al.* Efficient solar cells based on an easily accessible diketopyrrolopyrrole polymer. *Adv. Mater.* **22,** E242–E246 (2010).
18. Piliego, C. *et al.* Synthetic control of structural order in *n*-alkylthieno[3,4-*c*] pyrrole-4,6-dione-based polymers for efficient solar cells. *J. Am. Chem. Soc.* **132,** 7595–7597 (2010).
19. Yu, G., Gao, J., Hummelen, J. C., Wudl, F. & Heeger, A. J. Polymer photovoltaic cells: enhanced efficiencies via a network of internal donor–acceptor heterojunctions. *Science* **270,** 1789–1791 (1995).
20. Li, G., Chu, C.-W., Shrotriya, V., Huang, J. & Yang, Y. Efficient inverted polymer solar cells. *Appl. Phys. Lett.* **88,** 253503 (2006).
21. White, M. S. *et al.* Inverted bulk-heterojunction organic photovoltaic device using a solution-derived ZnO underlayer. *Appl. Phys. Lett.* **89,** 143517 (2006).
22. Liao, H-H. *et al.* Highly efficient inverted polymer solar cell by low temperature annealing of Cs_2CO_3 interlayer. *Appl. Phys. Lett.* **92,** 173303 (2008).
23. Shrotriya, V. *et al.* Efficient light harvesting in multiple-device stacked structure for polymer solar cells. *Appl. Phys. Lett.* **88,** 064104 (2006).
24. Padinger, F., Rittberger, R. S. & Sariciftci, N. S. Effects of postproduction treatment on plastic solar cells. *Adv. Funct. Mater.* **13,** 85–88 (2003).
25. Li, G. *et al.* High-efficiency solution processable polymer photovoltaic cells by self-organization of polymer blends. *Nat. Mater.* **4,** 864–868 (2005).
26. Peet, J. *et al.* Efficiency enhancement in low-bandgap polymer solar cells by processing with alkane dithiols. *Nature Mater.* **6,** 497–500 (2007).
27. Chen, H. Y. *et al.* Polymer solar cells with enhanced open-circuit voltage and efficiency. *Nature Photon.* **3,** 649–653 (2009).
28. Liang, Y. Y. *et al.* For the bright future—bulk heterojunction polymer solar cells with power conversion efficiency of 7.4%. *Adv. Mater.* **22,** E135–E138 (2010).

29. Chu, T. Y. *et al.* Bulk heterojunction solar cells using thieno[3,4-*c*]pyrrole- 4,6-dione and dithieno[3,2-*b*:2′,3′-*d*]silole copolymer with a power conversion efficiency of 7.3%. *J. Am. Chem. Soc.* **133,** 4250–4253 (2011).
30. Zhou, H. X. *et al.* Development of fluorinated benzothiadiazole as a structural unit for a polymer solar cell of 7% efficiency. *Angew. Chem. Int. Ed.* **50,** 2995–2998 (2011).
31. He, Z. *et al.* Simultaneous enhancement of open-circuit voltage, short-circuit current density and fill factor in polymer solar cells. *Adv. Mater.* **23,** 4636–4643 (2011).
32. Sista, S., Hong, Z. R., Chen, L. M. & Yang, Y. Tandem polymer photovoltaic cells—current status, challenges and future outlook. *Energy Environ. Sci.* **4,** 1606–1620 (2011).
33. Yang, J. *et al.* A robust inter-connecting layer for achieving high performance tandem polymer solar cells. *Adv. Mater.* **23,** 3465–3470 (2011).
34. Dennler, G. *et al.* Design rules for donors in bulk-heterojunction tandem solar cells—towards 15% energy-conversion efficiency. *Adv. Mater.* **20,** 579–583 (2008).
35. Scharber, M. C. *et al.* Design rules for donors in bulk-heterojunction solar cells—towards 10% energy-conversion efficiency. *Adv. Mater.* **18,** 789–794 (2006).
36. Huo, L. *et al.* Bandgap and molecular level control of the low-bandgap polymers based on 3,6-dithiophen-2-yl-2,5-dihydropyrrolo[3,4-*c*]pyrrole-1,4-dione toward highly efficient polymer solar cells. *Macromolecules* **42,** 6564–6571 (2009).
37. Huo, L. J. *et al.* A polybenzo[1,2-*b*:4,5-*b*′]dithiophene derivative with deep HOMO level and its application in high-performance polymer solar cells. *Angew. Chem. Int. Ed.* **49,** 1500–1503 (2010).
38. Shrotriya, V. *et al.* Accurate measurement and characterization of organic solar cells. *Adv. Funct. Mater.* **16,** 2016–2023 (2006).
39. Bijleveld, J. C. *et al.* Poly(diketopyrrolopyrrole-terthiophene) for ambipolar logic and photovoltaics. *J. Am. Chem. Soc.* **131,** 16616–16617 (2009).
40. Huo, L. J. *et al.* Replacement of alkoxy with alkylthienyl: a feasible approach to improve photovoltaic properties of PBDTTT-based polymers. *Angew. Chem. Int. Ed.* **50,** 1–7 (2011).
41. Coffin, R. C., Peet, J., Rogers, J. & Bazan, G. C. Streamlined microwave-assisted preparation of narrow-bandgap conjugated polymers for high performance bulk heterojunction solar cells. *Nature Chem.* **1,** 657–661 (2009).
42. He, Y. J., Chen, H.-Y., Hou, J. H. & Li, Y. F. Indene−C_{60} bisadduct: a new acceptor for high-performance polymer solar cells. *J. Am. Chem. Soc.* **132,** 1377–1382 (2010).
43. Burdick, J. & Glatfelter, T. Spectral response and *I–V* measurements of tandem amorphous-silicon alloy solar cells. *Solar Cells* **18,** 301–314 (1986).
44. Gilot, J., Wienk, M. M. & Janssen, R. A. J. Measuring the external quantum efficiency of two-terminal polymer tandem solar cells. *Adv. Funct. Mater.* **20,** 3904–3911 (2010).
45. Sun, B. Q. & Sirringhaus, H. Solution-processed zinc oxide field-effect transistors based on self-assembly of colloidal nanorods. *Nano Lett.* **5,** 2408–2413 (2005).
46. Beek, W. J. E., Wienk, M. M. & Janssen, R. A. J. Efficient hybrid solar cells from zinc oxide nanoparticles and a conjugated polymer. *Adv. Mater.* **16,** 1009–1013 (2004).
47. Meusel, M. *et al.* Spectral response measurements of monolithic GaInP/Ga(In)As/Ge triple-junction solar cells: measurement artifacts and their explanation. *Prog. Photovolt. Res. Appl.* **11,** 499–514 (2003).

Acknowledgements

This work was financially supported by the National Science Foundation (NSF, grant no. CHE0822573; programme manager: C. Foss), the Air Force Office of Scientific Research (AFOSR, grant no. FA9550-09-1-0610; programme manager: C. Lee) and the Office of Naval Research (ONR, grant no. N00014-04-1-0434; programme manager: P. Armistead), as well as by the US Department of Energy (contract no. DE-AC36-08-GO28308) together with the National Renewable Energy Laboratory. The authors thank R. Green, E. Richard, W.B. Yang and W.-C. Hsu of the Department of Materials Science and Engineering at UCLA for material testing, synthesis, ultraviolet photoelectron spectroscopy and X-ray diffraction measurements, respectively. Thanks also go to K.N. Houk and B. Martin of the Department of Chemistry (UCLA) for the quantum chemical calculation and R. Kaner and P. Weiss of the Department of Chemistry (UCLA) for reading the manuscript.

Author contributions

L.D. and J.You contributed equally to this work. L.D., J.You and Y.Y. developed the ideas. L.D. designed the chemical structure and performed materials synthesis and characterization. J.You fabricated the inverted tandem device and carried out data analysis. Y.H. and J.Yang participated in material synthesis and characterization. S.M. provided the ZnO for ICL. C.C. modified the PEDOT for ICL. T.M. and K.E. performed the certification at NREL. G.L. guided device testing at UCLA and coordinated certification. L.D., J.You, G.L. and Y.Y. prepared the manuscript. All authors discussed the results and commented on the manuscript. Y.Y. planned and supervised the project.

Additional information

The authors declare no competing financial interests. Supplementary information accompanies this paper at www.nature.com/naturephotonics. Reprints and permission information is available online at http://www.nature.com/reprints. Correspondence and requests for materials should be addressed to Y.Y.